Science
AAAS

Single-Molecule Torsional Pendulum
Jannik C. Meyer, *et al.*
Science **309**, 1539 (2005);
DOI: 10.1126/science.1115067

Science (print ISSN 0036-8075; online ISSN 1095-9203) is published weekly, except the last week in December, by the American Association for the Advancement of Science, 1200 New York Avenue NW, Washington, DC 20005.

diverged from the ADAT2/3 family by acquiring the ability to bind IP_6, followed by the acquisition of one or more dsRBMs to generate an ADAR. ADAT1 may have evolved an IP_6 binding function as a means of regulation. IP_6 accumulates in yeast during times of stress (*39*) and thus could lead to increased ADAT1 activity, and consequently to an increased conversion of A37 to N^1-methylinosine. Modification of position 37 is predicted to increase fidelity of protein synthesis by stabilizing the codon-anticodon interaction (*40*), and thus yeast may use this modification to fine-tune protein synthesis in response to environmental conditions.

Once established as a means of regulation for ADAT1, metazoa may have extended this regulatory mode for use in ADARs, which perform important roles in the nervous system and display changes in activity during development (*41*). For example, a feedback mechanism could act through phospholipase C in response to hormones such as serotonin. Upon binding of serotonin to its $5\text{-}HT_{2c}$ receptor, phospholipase C is activated to cleave phosphatidyl inositol 4,5-bisphosphate (PIP_2) to form the second messengers diacylglycerol and inositol 1,4,5-triphosphate (IP_3), which is subsequently phosphorylated to form IP_6. $5\text{-}HT_{2C}$ receptor mRNA is edited at five distinct sites by ADAR2, with the more extensively modified receptors requiring greater concentrations of serotonin to stimulate phospholipase C. It is tempting, therefore, to speculate that the serotonin-induced production of IP_6 causes increased production of active ADAR2, which in turn edits mRNA to attenuate the serotonin signaling pathway.

The structure of the hADAR2 catalytic domain reveals the active site architecture of a zinc-catalyzed deamination reaction and suggests how ADARs discriminate between cytidine and adenosine residues. The presence of IP_6 in the protein core implied an unexpected requirement for this cofactor in ADARs, which was confirmed by assaying the RNA editing activity of enzymes lacking IP_6. The finding that IP_6 is required for ADAR and ADAT activity suggests many interesting links between RNA editing and diverse processes such as cell signaling and translation, thus setting the stage for future studies.

References and Notes

1. B. L. Bass, *Annu. Rev. Biochem.* **71**, 817 (2002).
2. M. Higuchi *et al.*, *Nature* **406**, 78 (2000).
3. M. J. Palladino, L. P. Keegan, M. A. O'Connell, R. A. Reenan, *Cell* **102**, 437 (2000).
4. L. A. Tonkin *et al.*, *EMBO J.* **21**, 6025 (2002).
5. S. W. Knight, B. L. Bass, *Mol. Cell* **10**, 809 (2002).
6. A. D. Scadden, C. W. Smith, *EMBO Rep.* **2**, 1107 (2001).
7. L. A. Tonkin, B. L. Bass, *Science* **302**, 1725 (2003).
8. S. Maas, A. Rich, K. Nishikura, *J. Biol. Chem.* **278**, 1391 (2003).
9. T. Melcher *et al.*, *Nature* **379**, 460 (1996).
10. C. M. Burns *et al.*, *Nature* **387**, 303 (1997).
11. S. M. Rueter, T. R. Dawson, R. B. Emeson, *Nature* **399**, 75 (1999).
12. M. A. O'Connell, A. Gerber, W. Keller, *J. Biol. Chem.* **272**, 473 (1997).
13. M. R. Macbeth, A. T. Lingam, B. L. Bass, *RNA* **10**, 1563 (2004).
14. Materials and methods are available as supporting material on *Science* Online.
15. L. Betts, S. Xiang, S. A. Short, R. Wolfenden, C. W. Carter Jr., *J. Mol. Biol.* **235**, 635 (1994).
16. M. Kuratani *et al.*, *J. Biol. Chem.* **280**, 16002 (2005).
17. U. Kim, Y. Wang, T. Sanford, Y. Zeng, K. Nishikura, *Proc. Natl. Acad. Sci. U.S.A.* **91**, 11457 (1994).
18. A. P. Gerber, W. Keller, *Trends Biochem. Sci.* **26**, 376 (2001).
19. A. G. Polson, B. L. Bass, *EMBO J.* **13**, 5701 (1994).
20. O. M. Stephens, H. Y. Yi-Brunozzi, P. A. Beal, *Biochemistry* **39**, 12243 (2000).
21. X. Cheng, R. J. Roberts, *Nucleic Acids Res.* **29**, 3784 (2001).
22. J. W. Schwabe, A. Klug, *Nat. Struct. Biol.* **1**, 345 (1994).
23. J. E. Wedekind, P. A. Frey, I. Rayment, *Biochemistry* **34**, 11049 (1995).
24. D. C. Carlow, C. W. Carter Jr., N. Mejlhede, J. Neuhard, R. Wolfenden, *Biochemistry* **38**, 12258 (1999).
25. J. D. York, A. R. Odom, R. Murphy, E. B. Ives, S. R. Wente, *Science* **285**, 96 (1999).
26. L. A. Hanakahi, S. C. West, *EMBO J.* **21**, 2038 (2002).
27. M. Hoy *et al.*, *Proc. Natl. Acad. Sci. U.S.A.* **99**, 6773 (2002).
28. X. Shen, H. Xiao, R. Ranallo, W. H. Wu, C. Wu, *Science* **299**, 112 (2003).
29. D. J. Steger, E. S. Haswell, A. L. Miller, S. R. Wente, E. K. O'Shea, *Science* **299**, 114 (2003).
30. B. Valastro *et al.*, *Hippocampus* **11**, 673 (2001).
31. V. Raboy, *Phytochemistry* **64**, 1033 (2003).
32. A. Gerber, H. Grosjean, T. Melcher, W. Keller, *EMBO J.* **17**, 4780 (1998).
33. H. Grosjean *et al.*, *Biochimie* **78**, 488 (1996).
34. A. P. Gerber, W. Keller, *Science* **286**, 1146 (1999).
35. A. Saiardi, J. J. Caffrey, S. H. Snyder, S. B. Shears, *J. Biol. Chem.* **275**, 24686 (2000).
36. M. Kroger, B. Singer, *Biochemistry* **18**, 3493 (1979).
37. A. Arnone, M. F. Perutz, *Nature* **249**, 34 (1974).
38. B. M. Collins, A. J. McCoy, H. M. Kent, P. R. Evans, D. J. Owen, *Cell* **109**, 523 (2002).
39. P. P. Ongusaha, P. J. Hughes, J. Davey, R. H. Mitchell, *Biochem. J.* **335**, 671 (1998).
40. H. Grosjean, C. Houssier, P. Romby, R. Marquet, in *Modification and Editing of RNA*, H. Grosjean, R. Benne, Eds. (ASM Press, Washington, DC, 1998), pp. 113–134.
41. H. Lomeli *et al.*, *Science* **266**, 1709 (1994).

42. Single-letter abbreviations for the amino acid residues are as follows: A, Ala; C, Cys; D, Asp; E, Glu; F, Phe; G, Gly; H, His; I, Ile; K, Lys; L, Leu; M, Met; N, Asn; P, Pro; Q, Gln; R, Arg; S, Ser; T, Thr; V, Val; W, Trp; and Y, Tyr.

43. C. X. Chen *et al.*, *RNA* **6**, 755 (2000).

44. We thank R. Schackmann for synthesis of oligonucleotides and N-terminal sequencing and C. Nelson for mass spectrometry analysis; both are supported by a Cancer Center Support Grant (2P30CA042014). We also thank P. Beal and S. Wente for helpful discussions. This work was supported by grants from the National Institute of General Medical Sciences, GM44073 and GM56775, to B.L.B. and C.P.H., respectively. A.P.V. is supported by a postdoctoral fellowship from the American Cancer Society. B.L.B. is a Howard Hughes Medical Institute Investigator.

Supporting Online Material

www.sciencemag.org/cgi/content/full/309/5740/1534/DC1
Materials and Methods
Figs. S1 to S8
Tables S1 and S2
References

4 April 2005; accepted 29 July 2005
10.1126/science.1113150

REPORTS

Single-Molecule Torsional Pendulum

Jannik C. Meyer,[1]* Matthieu Paillet,[2] Siegmar Roth[1]

We have built a torsional pendulum based on an individual single-walled carbon nanotube, which is used as a torsional spring and mechanical support for the moving part. The moving part can be rotated by an electric field, resulting in large but fully elastic torsional deformations of the nanotube. As a result of the extremely small restoring force associated with the torsional deformation of a single molecule, unusually large oscillations are excited by the thermal energy of the pendulum. By diffraction analysis, we are able to determine the handedness of the molecule in our device. Mechanical devices with molecular-scale components are potential building blocks for nanoelectromechanical systems and may also serve as sensors or actuators.

Carbon nanotubes (*1*, *2*) are likely to be used in future nanoscale devices because of their outstanding mechanical and electrical properties. Nanoelectromechanical devices incorporating multiwalled carbon nanotubes (MWNTs) as motion-enabling elements have been demonstrated; in these devices, the MWNT serves as a torsional spring for small angular deformations (*3*) and torsional oscillations (*4*) or as a bearing for continuous rotational operation (*5*, *6*). Here, we show that it is possible to prepare large moving objects suspended on a single molecule—a single-walled nanotube (SWNT). The cross-section of a SWNT is smaller than that of a MWNT by more than two orders of magnitude, and large deformations are possible within the elastic regime. The moving part returns to its initial position even after being turned by 180°. The ultralow torsional spring constant provided by the

[1]Max Planck Institute for Solid State Research, D-70569 Stuttgart, Germany. [2]Laboratoire des Colloïdes, Verres et Nanomatériaux, Université de Montpellier II, 34095 Montpellier, France.

*To whom correspondence should be addressed. E-mail: j.meyer@fkf.mpg.de

SWNT allows for an easily detected deflection of the pendulum from excitations as small as those from the thermal energy.

Individual SWNTs are grown on a silicon substrate with a 200-nm oxide layer by chemical vapor deposition (*7*). The tubes are located with respect to a marker structure by atomic force microscopy. The device structure, consisting of 100 nm of Au with a 3-nm Cr adhesion layer, is prepared by electron beam lithography. The substrate is cleaved so that the structure is close (<10 μm) to a cleaved edge, as illustrated in Fig. 1. These structures are etched first in 15% tetramethylammonium hydroxide (TMAH) solution for several hours. The TMAH removes the bulk silicon and undercuts the structure from the side of the cleaved edge. As a result, the structure and the oxide layer reach out across the side edge of the substrate. The TMAH etching process is monitored with an optical microscope until a sufficient part of the structure is free-standing. Afterward, buffered hydrofluoric acid is used to remove the oxide layer, followed by critical-point drying.

The advantage of preparing a free-standing structure on the corner of a substrate is that it is accessible by a transmission electron microscope (TEM). Using a similar process, we have recently combined TEM and transport measurements, including gate characteristics, on the same nanotube (*8*). Arbitrary free-standing structures can be designed in this way, and accessibility by TEM is important for understanding and optimizing novel nanoelectromechanical systems.

The devices shown in Figs. 2 and 3 consist of a metal block suspended on an individual SWNT. Although the key motion-enabling element here is a single molecule, the suspended object is large enough to be visible in an optical microscope. In the TEM, the pendulum shown in Fig. 2 is already turned by ~70° as a result of electrostatic charging from the electron beam. This effect would not affect the device in possible applications outside an electron microscope. The charging is attributed to the high-resistance contacts between the nanotube and the metal structure. It is not present in the device shown in Fig. 3, which can be actuated by an external field between the support of the pendulum and a nearby electrode. In all the investigated devices, the carbon nanotube acts as a torsional spring in a regime of fully elastic deformation. The pendulum turns back to the initial position once the potential is switched off, even though it was turned by 180°. This is one distinction from MWNT-based devices, which are reported to break the outer shells at a deflection of 20° (followed by a continuous rotational freedom) in a similar geometry.

The device in Fig. 3 has a mass of $m \approx 2 \times 10^{-16}$ kg and a moment of inertia of $J \approx 7 \times 10^{-30}$ kg·m^2 with respect to the tube axis. The torsional spring constant of the tube axis is $C \approx 3 \times 10^{-18}$ N·m per radian, calculated from values in (*9*), our device geometry, and a tube diameter of 1.5 nm. Therefore, a torsional pendulum built on a SWNT can be turned by extremely small forces. For a rotation of 1°, a torque of 5×10^{-20} N·m is necessary. This corresponds to a force of 0.1 pN acting on one end of the rotor 400 nm away from the axis. Such a deflection can be detected by optical means because the rotor is sufficiently large. Optical displacement sensing with nanometer sensitivity has been demonstrated for objects of similar size (*10*). More intriguing, however, is the possibility that the nanotube itself could be used to sense the deformation, because a torsional deformation is expected to strongly influence the tube's electronic structure (*11*).

Extremely small perturbances can also excite a visible torsional oscillation. The resonance frequency for the torsional oscillation is calculated to be $f = [1/(2\pi)][(C/J)^{1/2}] \approx 0.1$ MHz. We can observe the thermally excited oscillations at room temperature in the TEM as unsharp edges of the pendulum, also visible in Fig. 2C. The amplitude of an oscillation with an energy of $k_B T$ (where k_B is the Boltzmann constant and T is absolute temperature) is calculated to be 3° for the geometry of the device shown in Fig. 2, which has a nanotube diameter of 2.4 nm. In all investigated devices, the observed thermal vibrations are in good agreement with the cal-

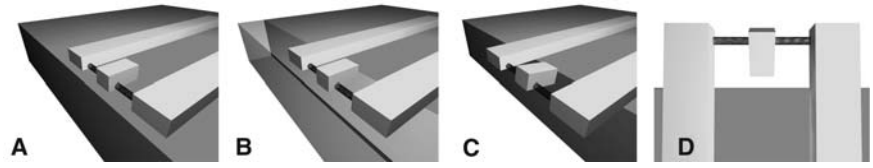

Fig. 1. Principle of sample preparation. (**A**) The structure is prepared on top of the nanotubes by electron beam lithography close to a cleaved edge of a substrate. (**B**) An etching process removes part of the substrate. (**C**) The part of the structure reaching out across the side edge is now free to move. (**D**) A view from the top shows that it is accessible by the TEM.

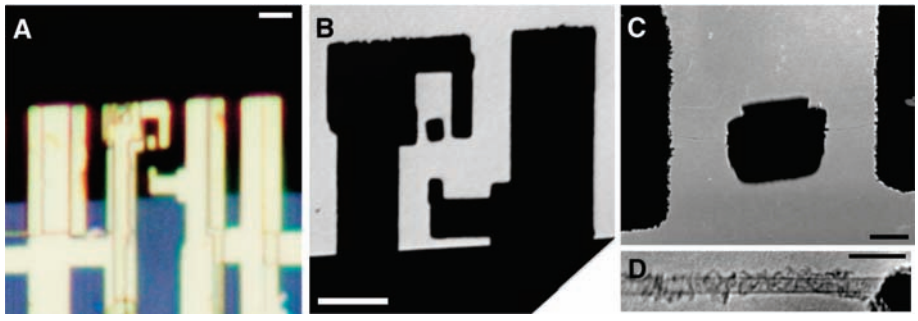

Fig. 2. A metal block suspended on one individual SWNT. (**A**) The metal block is visible in an optical microscope. (**B** and **C**) In the TEM, the suspended part rotates by up to ~70° as a result of charging by the electron beam with increasing magnification. (**D**) A high-resolution TEM image taken at the right end of the tube shows that this device is indeed built on one single molecule. Most of the amorphous carbon visible in (D) was deposited during the TEM analysis. Scale bars, 2 μm [(A) and (B)], 200 nm (C), 5 nm (D).

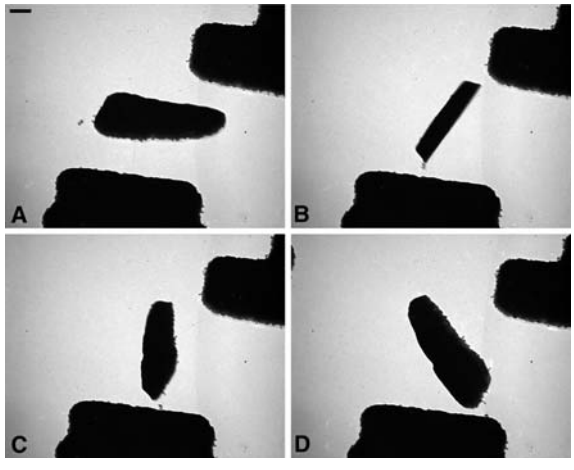

Fig. 3. A torsional pendulum built on a SWNT. (**A** to **D**) Images obtained at potentials of 0 V, 7.4 V, 9.7 V, and 22 V, respectively, between the support and the second electrode [visible in the upper left corner of (D)]. The sample is tilted by 30° for a slightly side-on view on the device. Scale bar, 100 nm. This device is also shown in movie S1.

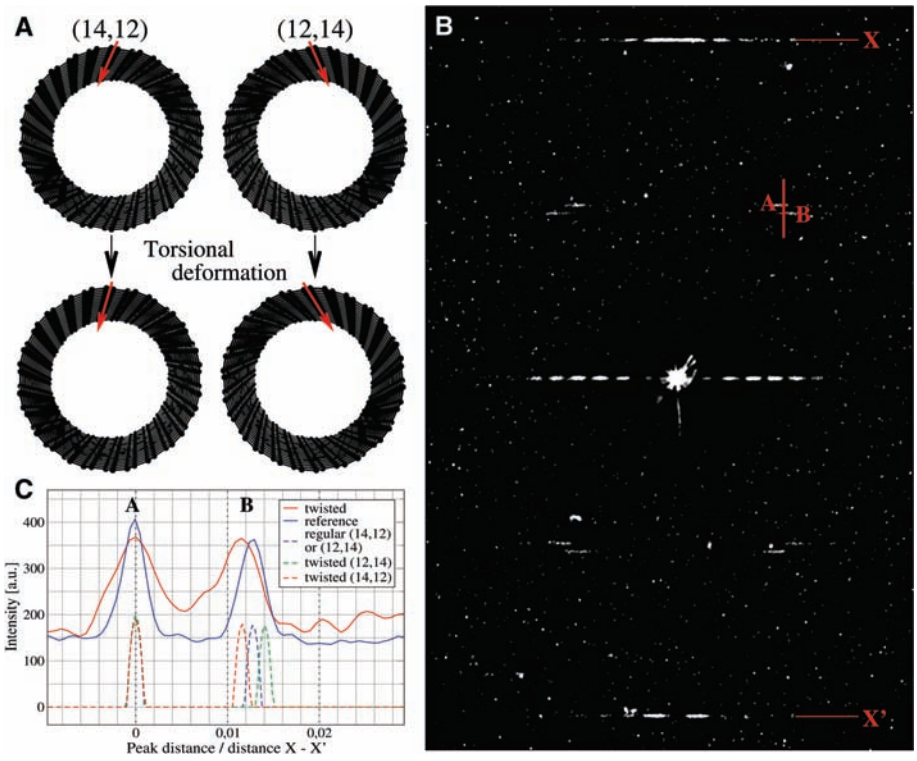

Fig. 4. (**A**) Effect of torsional deformation on the enantiomers of a (14,12) nanotube, viewed along the tube axis. The red arrows indicate a line along the graphene lattice, forming a right- or left-handed helix as it follows the cylindrical surface of the tube. The pitch of these helices is identical in the undeformed objects, but after a torsional deformation in a given direction, the pitch of the helices is different in the two enantiomers. The twisted (14,12) is no longer mirror-symmetric to the (12,14). (**B**) Diffraction pattern of a twisted nanotube. (**C**) Intensity profile along the A-B line in (B), as indicated in the pattern (solid red line) and for an undeformed (14,12) nanotube (solid blue line). Shown as dashed lines are simulated diffraction patterns of torsionally deformed nanotubes, twisted in the same direction and magnitude as in our device. The *x* axis is normalized to the distance between the layer lines denoted by X and X′ in (B). The angle between the tube axis and the graphene lattice can be precisely determined from the relative peak distances (*13*). All A peaks are plotted at $x = 0$. The clear difference in the peak distances, in agreement with the simulations, makes it possible to determine which enantiomer is present. Because the direction of the twist is known, we can determine that the tube structure (14,12), and not its mirror counterpart, is present in this device.

culated ones. The amplitude depends only on the diameter and length of the nanotube, not the geometry of the suspended object. Thermal vibrations up to 10° occur in devices with small-diameter (1 nm) nanotubes. The good agreement between observed and calculated values confirms that the modelization of the vibrational modes is valid and the nanotubes indeed exhibit the predicted mechanical properties.

Attaching a moving part with an individual SWNT is presumably one of the weakest couplings (i.e., one of the lowest spring constants) that can be realized. A pendulum on a SWNT 1.5 nm in diameter is supported by a total of only 40 C-C bonds (20 on each side), hence this approach is close to the limit (support by a single bond) that could be conceived for a mechanically attached object. If we consider the device as a quantum mechanical torsional harmonic oscillator, the angular uncertainty $\Delta\alpha$ of the quantum mechanical zero-point oscillation is of a magnitude $\Delta\alpha = \{[h/(2\pi)]/[(C \times J)^{1/2}]\}^{1/2}$ (where h is the Planck constant). For our device geometry, this angular uncertainty is 0.0003°, which corresponds to a position uncertainty of 2×10^{-12} m for the edge of the pendulum.

We note that a large position uncertainty requires not only a very small moving object (leading to a small mass and moment of inertia J) but also the weakest possible coupling (here in terms of the spring constant C). However, reaching a quantum-limited regime where $k_B T \approx hf$ would require microkelvin temperatures for our devices. To push the quantum limit to higher temperatures, it would be necessary to optimize the device geometry toward a higher resonance frequency (e.g., by reducing the size and mass of the moving object).

Figure 4B shows a diffraction pattern (*12*, *13*) obtained from a twisted SWNT on one side of a torsional pendulum. The tube section (300 nm in length) between the support and the rotated metal block is torsionally deformed, because one end of this tube section is turned by nearly 180°. By comparison with simulations, the nanotube can be identified as (14,12). However, there is a small deviation from the diffraction pattern of an undeformed (14,12) nanotube. In agreement with simulations for a torsionally deformed structure, this deviation shows that the tube is indeed homogeneously twisted (and not deformed, e.g., at a single defect).

Nanotubes (with the exception of the so-called armchair or zigzag types) are chiral molecules; that is, they are not identical with their mirror objects. Normally it is not possible to determine the handedness of a nanotube from a diffraction pattern. The diffraction pattern is the Fourier transform of the projected atomic potentials, and the (n,m) nanotube and its mirror counterpart [which we call (m,n)] have the same projected potential. In our case, however, the nanotube is torsionally deformed in a known direction. The two mirror-symmetric enantiomers, after deformation in a given direction, are no longer mirror-symmetric (Fig. 4A). Thus, it becomes possible to determine which type is present. From the deviation in the peak distances, we determine that in our device we have deformed the nanotube structure denoted as (14,12), and not its mirror counterpart.

Our SWNT pendulum can be reproducibly turned to any position between 0° and almost 180° with the use of a single electrostatic potential. Nanoelectromechanical systems applications include micromirrors or devices that require continuous tilting (with a precisely defined rotation axis) of any object attached to the nanotube or the pendulum. Because deflections and oscillations can be induced by extremely small forces, the pendulum can serve as a component in very sensitive nanoscale force sensors.

References and Notes

1. S. Iijima, *Nature* **354**, 56 (1991).
2. S. Iijima, T. Ichihashi, *Nature* **363**, 603 (1993).
3. P. A. Williams *et al.*, *Appl. Phys. Lett.* **82**, 805 (2003).
4. S. J. Papadakis *et al.*, *Phys. Rev. Lett.* **93**, 146101 (2004).
5. A. M. Fennimore *et al.*, *Nature* **424**, 408 (2003).
6. B. Bourlon, D. C. Glattli, C. Miko, L. Forro, A. Bachtold, *Nano Lett.* **4**, 709 (2004).
7. M. Paillet *et al.*, *J. Phys. Chem. B* **108**, 17112 (2004).
8. J. C. Meyer, D. Obergfell, S. Yang, S. Yang, S. Roth, *Appl. Phys. Lett.* **85**, 2911 (2004).
9. J. P. Lu, *Phys. Rev. Lett.* **79**, 1297 (1997).
10. D. W. Carr, S. Evoy, L. Sekaric, H. G. Craighead, J. M. Parpia, *Appl. Phys. Lett.* **75**, 920 (1999).
11. A. Pantano, D. M. Parks, M. C. Boyce, M. B. Nardelli, *J. Appl. Phys.* **96**, 6756 (2004).
12. J. C. Meyer, M. Paillet, G. S. Duesberg, S. Roth, *Ultramicroscopy*, in press (available at http://arxiv.org/cond-mat/0506356).
13. M. Gao *et al.*, *Appl. Phys. Lett.* **82**, 2703 (2003).
14. Supported by Studienstiftung des Deutschen Volkes (J.C.M.), Bundesministerium für Bildung und Forschung (BMBF) project INKONAMI, and EU projects CANAPE and CARDECOM.

Supporting Online Material

www.sciencemag.org/cgi/content/full/309/5740/1539/DC1
Movie S1

19 May 2005; accepted 27 July 2005
10.1126/science.1115067